ChemComm

COMMUNICATION

View Article Online
View Journal | View Issue

Cite this: *Chem. Commun.*, 2025, **61**, 6126

Received 4th February 2025,
Accepted 18th March 2025

DOI: 10.1039/d5cc00625b

rsc.li/chemcomm

Effect of nanosizing on sodium cobalt(II) hexacyanoferrate(II) nanoparticles in nanofibers for enhanced ammonium adsorption capacity†

Makoto Sasaki [ab] and Mitsuhiro Ebara *[ab]

In this study, sodium cobalt(II) hexacyanoferrate(II) (NaCoHCF) nanoparticles were synthesized and incorporated into electrospun nanofibers to enhance their ammonium adsorption capacity. We successfully synthesized nanosized NaCoHCF using microfluidics and incorporated it into the nanofibers. This resulted in an approximately three-fold improvement in adsorption performance compared to that of micro-sized NaCoHCF.

Ammonium (NH_4^+) is a crucial compound in the nitrogen cycle and is widely present in the environment owing to both natural processes and human activities.[1,2] However, excessive ammonium can cause severe toxicity in both the environment and living organisms. For example, in many vertebrates, an increase in ammonium concentration in the body can lead to acute ammonia poisoning, followed by convulsions and ultimately death.[3] This phenomenon is believed to result from its effects on the central nervous system.[4,5] Additionally, whereas ammonium serves as an essential nitrogen source for plants, excessive uptake has also been reported to induce ammonium toxicity in them.[6,7] To prevent toxicity associated with ammonium accumulation, technologies for removing it from wastewater, industrial effluent, soil, and even blood are of considerable importance.

Among various methods, adsorption is known to be a highly effective method of removing ammonium, and several ammonium adsorbents—including zeolites and activated carbon—have been developed.[8–13] Among these, sodium cobalt(II) hexacyanoferrate(II) (NaCoHCF), as reported by Y. Jiang *et al.* in 2018, has attracted considerable attention owing to its exceptionally high ammonium adsorption capacity *via* ion exchange reactions, as well as its high selectivity for ammonium, making it a promising material for various applications.[14] Rather than using NaCoHCF in powder form, incorporating it into a substrate to create a filter offers several advantages, including the prevention of powder leakage, enhanced reusability, and multifunctional capabilities. However, when powdered adsorbents are used in liquid media, aggregation can occur, potentially reducing the adsorption efficiency. Nonetheless, incorporating NaCoHCF into a filter can help prevent aggregation and maintain the adsorption performance.

In this study, electrospun nanofibers were selected as substrates for incorporating NaCoHCF. Electrospinning is a technique for fabricating nanofibers through the application of a high voltage while extruding a polymer solution through a needle from a syringe. This method not only allows for the simple fabrication of nanofibers but also has the advantage of being able to produce nanofibers from various polymers by optimizing multiple parameters—such as the solution concentration, applied voltage, injection distance, and flow rate.[15] Additionally, nanofibers produced by electrospinning exhibit extremely fine fiber diameters and high specific surface areas, which are considered to be beneficial for ammonium adsorption.[16–18] In our previous study, nanofibers containing micro-sized NaCoHCF were fabricated *via* electrospinning and their ability to adsorb ammonium from solution was successfully demonstrated.[19] However, the micro-sized NaCoHCF particles were entangled with multiple nanofibers due to their size. Therefore, it was hypothesized that if nanosized NaCoHCF could be incorporated within a single nanofiber, more efficient adsorption could be realized. To achieve this, it would be necessary to synthesize NaCoHCF with particle sizes smaller than the fiber diameter.

In this study, we focused on the synthesis of NaCoHCF nanoparticles and their incorporation into nanofibers to improve their ammonium adsorption performance. Two different synthesis methods were employed to compare the NaCoHCF microparticles (micro-NaCoHCF) and NaCoHCF nanoparticles (nano-NaCoHCF). Micro-NaCoHCF was synthesized by mixing aqueous solutions of $Na_4[Fe(CN)_6]\cdot 10H_2O$ and $Co(NO_3)_2\cdot 6H_2O$ in a beaker under stirring, followed by freeze-drying of the resulting particle dispersion. By contrast, nano-NaCoHCF was obtained by mixing the two aqueous solutions within a Y-shaped microchannel, with

[a] *Research Center for Macromolecules and Biomaterials, National Institute for Materials Science (NIMS), 1-1 Namiki, Tsukuba, Ibaraki, 305-0044, Japan. E-mail: EBARA.Mitsuhiro@nims.go.jp*
[b] *Graduate School of Pure and Applied Sciences, University of Tsukuba, 1-1-1 Tennodai, Tsukuba, Ibaraki, 305-8577, Japan*

† Electronic supplementary information (ESI) available. See DOI: https://doi.org/10.1039/d5cc00625b

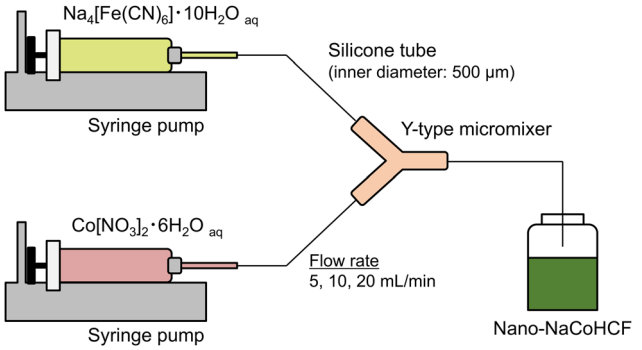

Fig. 1 Illustration of the experimental set-up for the synthesis of nano-NaCoHCF.

the particles forming during the process, followed by freeze-drying of the obtained dispersion (Fig. 1).

In this synthesis method, turbulence can occur when the two solutions collide, promoting nucleation and suppressing particle growth, thereby enabling the synthesis of nanoparticles. The synthesized micro- and nano-NaCoHCFs can then be incorporated into poly(ethylene-*co*-vinyl alcohol) (EVOH) nanofibers *via* electrospinning. The incorporation state can be observed using scanning electron microscopy (SEM) and transmission electron microscopy (TEM), followed by an ammonium adsorption test to evaluate the adsorption performance.

In this study, the particle sizes of the synthesized micro- and nano-NaCoHCF were measured using dynamic light scattering (DLS), the results of which are presented in Fig. 2(a) and (b). The average particle sizes calculated using the cumulant method were 4473.2 and 45.9 nm, respectively, confirming that the nano-NaCoHCF had a particle size approximately 1/100th that of the micro-NaCoHCF. Additionally, the nano-NaCoHCF exhibited a lower polydispersity index (PDI), suggesting that the particles were monodispersed. This was likely owing to turbulence during the mixing of the two solutions in the microchannel, leading to the formation of multiple locally supersaturated regions that enhanced nucleation. Consequently, a large portion of the solute was consumed during nucleation, suppressing particle growth and resulting in smaller particle sizes and lower PDI values.[20] Moreover, synthesis was conducted with various flow rates of the mixed solutions; however, particles of approximately 50 nm were obtained regardless of the flow rate, indicating no major change owing to flow rate variations (Fig. S1, ESI†). The minimum flow rate used in this study was 5 mL min^{-1}. However, even under these conditions, sufficient turbulence was achieved to facilitate nanoparticle synthesis. A previous study by Yamamoto *et al.* also reported that the particle size of ZIF-8 decreases with increasing flow velocity during mixing, but above a certain flow velocity, there is no change in particle size.[21]

NaCoHCF SEM images are presented in Fig. 2(c)–(f). The SEM images confirmed that the nano-NaCoHCF had a smaller particle size than the micro-NaCoHCF. However, the nano-NaCoHCF particle size observed in the SEM images was approximately 200 nm, which was larger than that from the DLS measurement results. This discrepancy was likely because

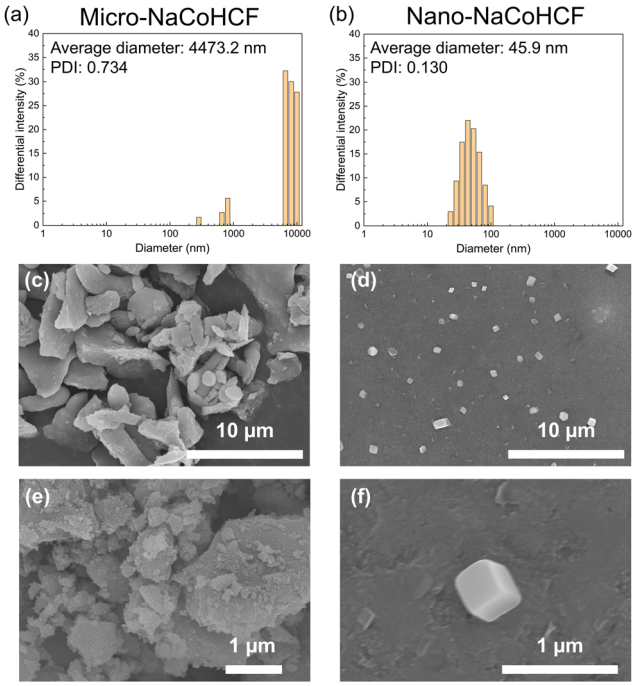

Fig. 2 (a) and (b) Intensity-weighted size distributions of the micro-NaCoHCF and nano-NaCoHCF particles measured by dynamic light scattering (DLS). The average diameters and polydispersion index (PDI) were calculated using the cumulant method. (c)–(f) SEM images of the synthesized NaCoHCF particles. (c) Micro-NaCoHCF with low magnification, (d) nano-NaCoHCF with low magnification, (e) micro-NaCoHCF with high magnification, and (f) nano-NaCoHCF with high magnification.

of particle aggregation that occurred during the drying of the nano-NaCoHCF dispersion, which was necessary for SEM sample preparation. Moreover, owing to the resolution limitations of SEM, the accurate observation of the nano-NaCoHCF morphology can be challenging. Consequently, additional observations were made using TEM (Fig. S2, ESI†), which revealed the presence of particles of approximately 100 nm in size and cubic structures constituting the particles themselves. Because NaCoHCF has been reported to have a cubic crystal structure, it could be inferred that these crystals aggregated to form the observed particles.

Nanofibers containing micro- and nano-NaCoHCF were fabricated using electrospinning, the SEM images of which are shown in Fig. 3(a) and (b). In the EVOH/micro-NaCoHCF nanofiber, inclusions of approximately 20–50 μm diameter could be observed, which were presumed to be micro-NaCoHCF. Instead of being embedded within the nanofibers, the micro-NaCoHCF particles were present on the nanofiber sheet, which was covered by a thin polymer layer. By contrast, no such inclusions were evident in the EVOH/nano-NaCoHCF nanofibers. Because the nano-NaCoHCF particle size was smaller than the nanofiber diameter, it could be inferred that the nano-NaCoHCF had been incorporated into the nanofibers.

To verify this, TEM imaging was conducted, the results of which are shown in Fig. 3(c). Inclusions were evident within the nanofibers and elemental analysis using energy-dispersive X-ray spectroscopy (EDX) confirmed the presence of Fe and Co

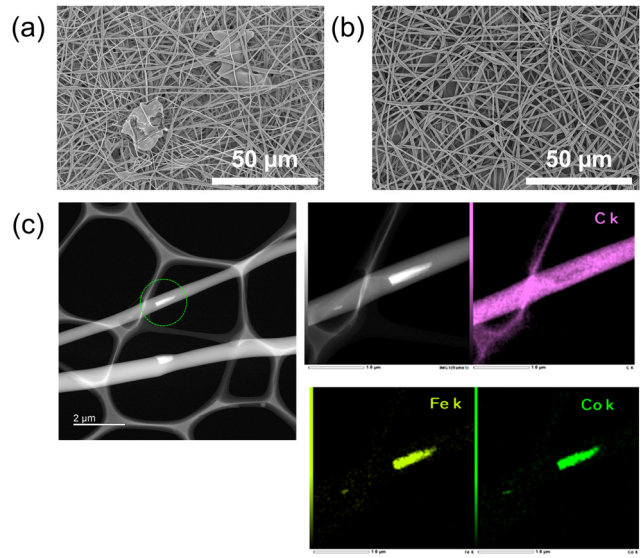

Fig. 3 (a) SEM image of the EVOH/micro-NaCoHCF nanofibers. (b) SEM image of the EVOH/nano-NaCoHCF nanofibers. (c) EDX mapping of the EVOH/nano-NaCoHCF nanofibers.

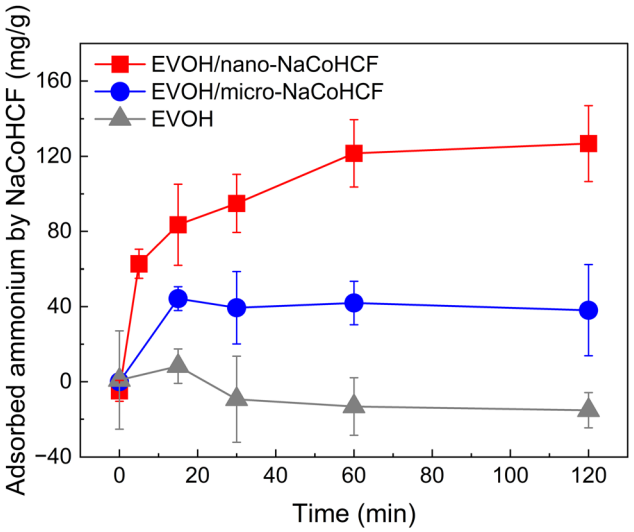

Fig. 4 Change of ammonium adsorption capacity of NaCoHCF in the EVOH/micro-NaCoHCF and EVOH/nano-NaCoHCF nanofibers (n = 3).

atoms in these inclusions. As the EVOH contained only carbon and oxygen atoms, the detected iron and cobalt atoms evidently originated from the NaCoHCF. These findings suggest that the nano-NaCoHCF had been successfully incorporated into the nanofibers.

Thermogravimetry/differential thermal analysis (TG/DTA) was performed to determine the NaCoHCF content of the EVOH/nano-NaCoHCF nanofibers and EVOH/micro-NaCoHCF nanofibers (Fig. S3, ESI†). In the thermogravimetric curves, both nano-NaCoHCF and micro-NaCoHCF showed similar mass loss behavior, suggesting that both have similar thermal tolerance. The NaCoHCF content in the nanofibers was calculated from the final residual mass to be 48.6 wt% for EVOH/nano-NaCoHCF and 51.5 wt% for EVOH/micro-NaCoHCF, confirming that the content was almost the same as the preparation ratio.

To evaluate the effect of the NaCoHCF particle size on the ammonium adsorption performance, adsorption tests were conducted using EVOH/micro-NaCoHCF and EVOH/nano-NaCoHCF nanofibers, the results of which are shown in Fig. 4.

The amount of ammonium adsorbed per unit mass of NaCoHCF did not increase for the EVOH nanofibers alone, confirming that the EVOH nanofibers possessed no ammonium adsorption capability. By contrast, both the EVOH/micro-NaCoHCF and EVOH/nano-NaCoHCF nanofibers exhibited an increase in ammonium adsorption over time—that is, after 2 h of testing, the ammonium adsorption amounts were 38.1 and 126.8 mg g^{-1}, respectively. The nano-NaCoHCF exhibited more than three times the adsorption performance of the micro-NaCoHCF. This result could be attributed to the higher specific surface area of the nano-NaCoHCF. In the case of the micro-NaCoHCF, ammonium was likely adsorbed only onto surface adsorption sites, with the internal adsorption sites not being utilized efficiently. By contrast, the nano-NaCoHCF—with its higher specific surface area—permitted increased utilization of the adsorption sites, leading to enhanced ammonium adsorption performance. Previous studies also observed that smaller particle sizes resulted in higher adsorption performance, consistent with the findings of this study.[22] Furthermore, in a paper published by H. Ming *et al.* in 2012, Prussian blue nanoparticles of different sizes were synthesized. For nanoparticles of the same size as those in our report, they reported a surface area of 254 m^2 g^{-1} and a pore diameter of around 8 nm.[23]

In summary, this study successfully synthesized nano-NaCoHCF particles of approximately 50 nm size and incorporated them into nanofibers. Consequently, the ammonium adsorption performance of the NaCoHCF within the nanofibers was considerably enhanced, exhibiting more than three times the adsorption capacity of the microparticles. This value surpassed those of commonly used ammonium adsorbents—such as zeolites (approximately 8–50 mg g^{-1})[10] and biochar (approximately 5–43 mg g^{-1})[8]—indicating that the material offered practical adsorption performance. Moreover, because the NaCoHCF was embedded within the nanofibers, the risk of leakage could be minimized, making it a promising candidate for various applications as an ammonium adsorption filter.

The findings of this study are not limited to NaCoHCF but are applicable to a wide range of adsorbent materials, suggesting the potential for further development of electrospun nanofiber/inorganic hybrid materials.

This work was supported by JSPS KAKENHI Grant Numbers JP20H05877 and JP23KJ0260. Part of this work was supported by "Advanced Research Infrastructure for Materials and Nanotechnology in Japan (ARIM)" of the Ministry of Education, Culture, Sports, Science and Technology (MEXT).

Data availability

The data supporting this article have been included as part of the ESI.†

Conflicts of interest

There are no conflicts to declare.

References

1 D. Fowler, M. Coyle, U. Skiba, M. A. Sutton, J. N. Cape, S. Reis, L. J. Sheppard, A. Jenkins, B. Grizzetti, J. N. Galloway, P. Vitousek, A. Leach, A. F. Bouwman, K. Butterbach-Bahl, F. Dentener, D. Stevenson, M. Amann and M. Voss, *Philos. Trans. R. Soc., B*, 2013, **368**, 20130164.
2 L. Y. Stein and M. G. Klotz, *Curr. Biol.*, 2016, **26**, R94–R98.
3 D. Randall and T. K. Tsui, *Mar. Pollut. Bull.*, 2002, **45**, 17–23.
4 M. D. Norenberg, K. V. Rama Rao and A. R. Jayakumar, *Metab. Brain Dis.*, 2009, **24**, 103–117.
5 M. Skowrońska and J. Albrecht, *Neurochem. Int.*, 2013, **62**, 731–737.
6 T. Hachiya, J. Inaba, M. Wakazaki, M. Sato, K. Toyooka, A. Miyagi, M. Kawai-Yamada, D. Sugiura, T. Nakagawa, T. Kiba, A. Gojon and H. Sakakibara, *Nat. Commun.*, 2021, **12**, 4944.
7 D. T. Britto, M. Y. Siddiqi, A. D. M. Glass and H. J. Kronzucker, *Proc. Natl. Acad. Sci. U. S. A.*, 2001, **98**, 4255–4258.
8 B. Han, C. Butterly, W. Zhang, J. He and D. Chen, *J. Cleaner Prod.*, 2021, **283**, 124611.
9 H. Huang, X. Xiao, B. Yan and L. Yang, *J. Hazard. Mater.*, 2010, **175**, 247–252.
10 J. Huang, N. R. Kankanamge, C. Chow, D. T. Welsh, T. Li and P. R. Teasdale, *J. Environ. Sci.*, 2018, **63**, 174–197.
11 H. Liu, Y. Dong, Y. Liu and H. Wang, *J. Hazard. Mater.*, 2010, **178**, 1132–1136.
12 M. Seredych, C. Petit, A. V. Tamashausky and T. J. Bandosz, *Carbon*, 2009, **47**, 445–456.
13 A. Alshameri, H. He, J. Zhu, Y. Xi, R. Zhu, L. Ma and Q. Tao, *Appl. Clay Sci.*, 2018, **159**, 83–93.
14 Y. Jiang, K. Minami, K. Sakurai, A. Takahashi, D. Parajuli, Z. Lei, Z. Zhang and T. Kawamoto, *RSC Adv.*, 2018, **8**, 34573–34581.
15 A. Keirouz, Z. Wang, V. S. Reddy, Z. K. Nagy, P. Vass, M. Buzgo, S. Ramakrishna and N. Radacsi, *Adv. Mater. Technol.*, 2023, **8** 1–34.
16 F. Ahmadijokani, H. Molavi, A. Bahi, R. Fernández, P. Alaee, S. Wu, S. Wuttke, F. Ko and M. Arjmand, *Adv. Funct. Mater.*, 2022, **32**, 1–67.
17 F. Haghdoost, S. H. Bahrami, J. Barzin and A. Ghaee, *Sep. Purif. Technol.*, 2021, **257**, 117881.
18 K. Namekawa, M. Tokoro Schreiber, T. Aoyagi and M. Ebara, *Biomater. Sci.*, 2014, **2**, 674.
19 M. Sasaki, L. Szabó, K. Uto and M. Ebara, *ACS Appl. Mater. Interfaces*, 2024, **16**, 67399–67410.
20 J. Lu, Y. Guo, B. Dong, X. Yang and J. Li, *Colloids Surf., A*, 2024, **694**, 134097.
21 D. Yamamoto, T. Maki, S. Watanabe, H. Tanaka, M. T. Miyahara and K. Mae, *Chem. Eng. J.*, 2013, **227**, 145–150.
22 Z. Jin, S. Xiao, H. Dong, J. Xiao, R. Tian, J. Chen, Y. Li and L. Li, *J. Hazard. Mater.*, 2022, **422**, 126928.
23 H. Ming, N. L. K. Torad, Y.-D. Chiang, K. C. W. Wu and Y. Yamauchi, *CrystEngComm*, 2012, **14**, 3387.